# Optical cells with fused silica windows for the study of geological fluids

#### I-MING CHOU

954 National Center, U.S. Geological Survey, Reston, VA 20192, U.S.A. e-mail: imchou@usgs.gov

Two types of optical cells with fused silica windows are described for study of geological fluids at temperatures (T) up to  $600^{\circ}$ C and pressures (P) up to 1 kbar. One is the high-pressure optical cell (HPOC), in which fluids of known composition can be loaded directly into the cell and its pressure can be adjusted and measured. The other is the fused silica capillary capsule (FSCC), which contains sample fluid with both ends of the tube flame sealed. Both types of cells can be inserted into a heatingcooling stage (USGS-type, the newly developed stage from INSTEC or that from Linkam) for in situ observations and Raman spectroscopic analyses at various P-T conditions. The HPOC has been applied to measure the solubility and diffusion of methane in water, the solubility of methane hydrate in water, and methane pressures in fluid samples. It is also very useful for providing fluid standards with known composition and pressure for the calibration of Raman spectroscopic systems before quantitative analyses. The FSCC is particularly useful for samples which need to be reacted at elevated P-T conditions for long periods of time (days or weeks). These two types of optical cells with fused silica windows are particularly suitable for the study of organic systems and also for systems containing sulphur.

#### 1. Introduction

Various types of optical cells with silica windows have been used previously, together with Raman spectroscopy, to study fluids but with only limited success. For example, Irish  $et\ al.$  (1982) developed a furnace assembly together with a sample cell constructed from thick-walled Corning Pyrex glass capillary tubing (7.5 mm OD, 1.5 mm ID) for vibrational spectral studies of solutions. Their cell could only be operated at temperatures (T) of  $<350^{\circ}$ C and pressures (P) of <17.5 MPa, and they observed significant corrosion of the Pyrex glass even by pure water samples at elevated P-T conditions. The high-pressure optical cell designed by Chou  $et\ al.$  (1990), which combined a high-pressure valve with a fused silica tubing (3 mm OD, 1 mm ID), could be used for collecting Raman spectra of fluids at pressures up to 100 MPa, but sample temperatures were limited to near room T (Chou  $et\ al.$ , 1990; Seitz  $et\ al.$ , 1993, 1996). Similarly, the cell designed by Lin  $et\ al.$  (2007), which combined a high-pressure valve with a 3.2 mm thick glass window, could reach pressures up to 60 MPa, but sample temperatures were again limited to near room T (Lin  $et\ al.$ , 2007; Fall  $et\ al.$ , 2011).

Recent development of optical cells allows us to not only observe many geological processes at higher P-T conditions, but also characterize geological samples in the

DOI: 10.1180/EMU-notes.12.6

cells by using advanced spectroscopic tools, including Raman spectroscopy and synchrotron X-ray spectroscopy. In this chapter, optical cells with fused silica windows are introduced which are suitable for P-T conditions of sedimentary basins, hydrothermal systems, and low-grade metamorphism (up to  $\sim 1$  kbar and  $600^{\circ}$ C). The other type of optical cell using diamond windows, the hydrothermal diamond-anvil cell (HDAC), suitable for the study of samples at P-T conditions up to those near the Moho ( $\sim 3$  GPa and  $1000^{\circ}$ C), are presented by Schmidt & Chou (2012, this volume).

Two types of optical cells using fused silica windows will be discussed here. One is the high-pressure optical cell (HPOC; Chou *et al.*, 2005), in which one end of the fused silica capillary tube was sealed with a hydrogen flame, and the other, open end was connected to a pressure line through a high-pressure valve, such that fluids of known composition can be loaded directly into the cell and its pressure can be measured by using a pressure transducer connected to the pressure line. The other type is the fused silica capillary capsule (FSCC; Chou *et al.*, 2008a), containing sample fluids with both ends of the tube flame sealed. FSCCs are particularly useful when combined with a heating-cooling stage for *in situ* observations and also for samples that need to be reacted at elevated *P-T* conditions for long durations (days or weeks).

# 2. High-pressure optical cell (HPOC)

#### 2.1. Construction of HPOC

A square flexible fused silica-capillary tube (300 µm × 300 µm with cavities of  $100 \mu m \times 100 \mu m$  or  $50 \mu m \times 50 \mu m$ ), commercially available from Polymicro Technologies, LLC (www.polymicro.com), forms the optical window in this cell. This, or other available sizes (such as 150 µm OD and 30 or 75 µm ID with a circular crosssection) was epoxied inside a stainless steel high-pressure capillary tubing (1.59 mm OD, 0.76 mm ID, and 40 mm long), which was connected to a high-pressure valve by a sleeve-gland assembly (Fig. 1). The silica tubes were supplied with a polyimide coating (~15 µm thick). To provide clear windows for optical observation of samples in the tube, a section of this brown polyimide protection cover was removed using a hydrogen flame. However, to add extra strength to the silica tube, the polyimide layer over the section of the tube to be inserted into the stainless steel tube should not be removed (Fig. 1). To further protect the silica tube, especially under high internal pressure, a slightly longer stainless high-pressure capillary tube can be used to enclose the entire silica tube; however, in this case it is necessary to grind off parts of the stainless tube immediately above and below the windows (Fig. 1c). The stainless high-pressure capillary tubing, sleeve, gland, and high-pressure valve are available from the High Pressure Equipment Company (www.highpressure.com).

#### 2.2. Sample loading and pressurizing procedures

Figure 2 is a schematic diagram showing the sample loading and pressurizing system for Raman spectroscopic analysis of non-aqueous fluid samples. The procedures are as follows.

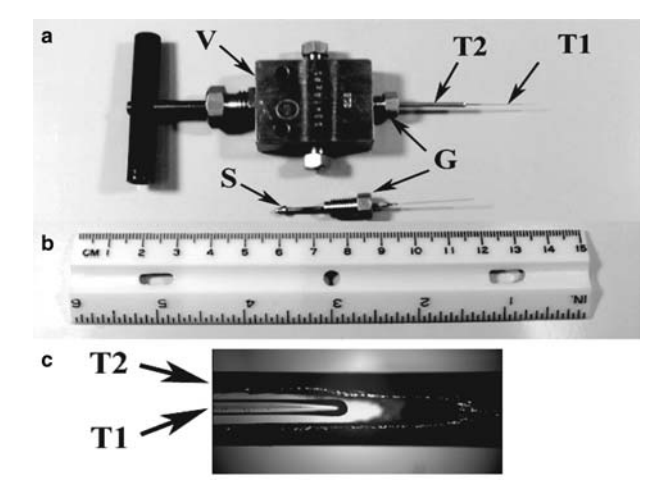


Fig. 1. Photograph of a high-pressure optical cell (HPOC). The following procedures were used to construct the HPOC as shown in (a): (1) remove the protection cover of polyimide at the window section of the square capillary tube (T-1) with a hydrogen flame; (2) seal this end of the tube with the hydrogen flame; (3) insert the other end of the tube through the high-pressure stainless steel tube (T-2), which already had a sleeve (S) and a gland (G) in place and filled with freshly mixed epoxy; (4) after the epoxy was set, cut off the end of the silica tube near the sleeve, and verify that the cavity was not blocked by epoxy; and (5) connect the assembly (b) to the high-pressure valve (V) as shown in (a). To protect the silica tube, a slightly longer stainless high-pressure capillary tube was used to enclose the entire silica tube, and parts of the stainless steel tube were ground away to expose the window, as shown in (c). Other kinds of protective tube with windows can be constructed to enclose the silica tube by sliding it along the stainless tube. An HPOC was also constructed with two open ends, and each end was connected to a high-pressure valve. This cell is slightly bulky, but it was much easier for cleaning and loading samples. However, make sure that the two valves are fixed in position, and that the distance between the two valves is slightly shorter than the silica tube in between, taking the advantage of the flexibility of the silica tube. The ruler shows scales in both centimetres and inches for (a) and (b). For scale in (c), the stainless tubing (T-2) is  $\sim$ 1.6 mm in OD. Part numbers: T-1 (Polymicro Technologies; 2001513, and 2001515), T2 (High Pressure Comp. (HiP); 15-9A1-030, 0.762 mm ID × 1.588 mm OD), V (HiP, 15-14AF1), G (HiP, 15-2AM1), and S (HiP, 15-2A1). Taken from figure 1 of Chou et al. (2005).

# (a) evacuate and flush the capillary cell and pressure line with sample fluid before loading

(1) close all valves; (2) open v-1, v-2, v-3, v-4 and v-5, and use the syringe (S-1) to evacuate the line; (3) close v-1 and open v-6 to load the line with the sample fluid from tank 1 (T-1), and use the pressure gauge (G-1) to read the pressure; (4) close v-6 and open v-1 to flush the line with the sample fluid; (5) after repeating the above steps several times, close v-1 and open v-6 to finally load the line with the sample fluid.

#### (b) load a section of water to separate sample fluid from the pressurizing fluid

(1) close v-2, v-5 and v-6; (2) open v-10 and v-11, and use the syringe (S-2) to fill the line between v-10 and v-11 with water, and then close v-10 and v-11.

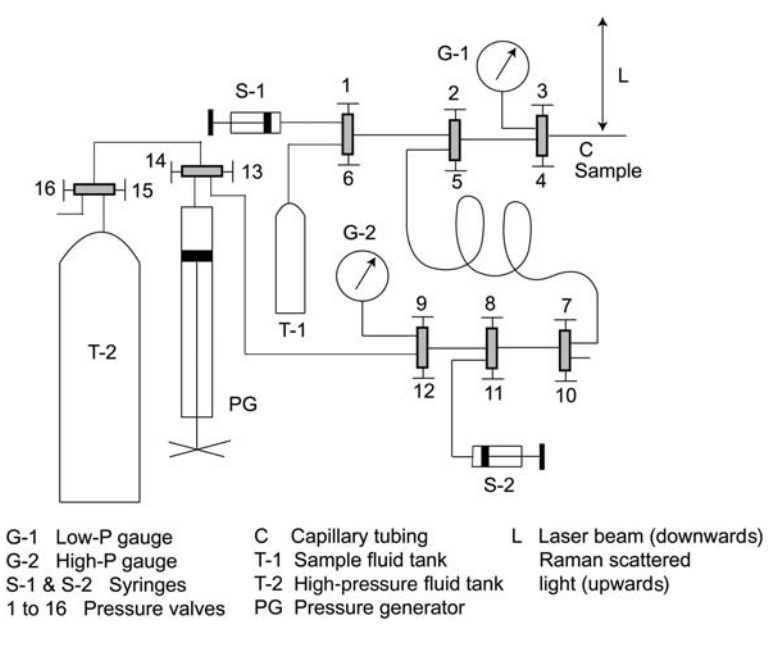


Fig. 2. Schematic diagram showing the sample loading and pressurization system for Raman spectroscopic analysis of fluid samples. For details, see text. Taken from figure 2 of Chou et al. (2005).

#### (c) Pressurize the sample

(1) open v-9, v-12, v-13 and v-14, and then open v-15 to load the line and pressure generator (PG) with a high-pressure fluid (CH<sub>4</sub>, N<sub>2</sub>, or CO<sub>2</sub>) from T-2; (2) close v-15 and open v-8 and v-7 to pressurize the sample fluid by pushing the water section between v-10 and v-11 into the loop between v-5 and v-7; (3) open v-5 and read the pressure of the sample fluid in the capillary tubing (C) (Fig. 3a when N<sub>2</sub> is used as the high-pressure fluid) at G-1 or G-2; (4) use the pressure generator to reach higher pressure, but close v-3 before reaching the maximum pressure rating for G-1; (5) close v-3, v-4

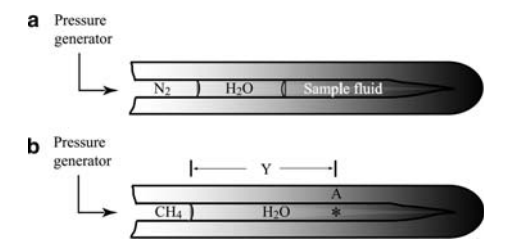


Fig. 3. Schematic diagrams showing (a) a small amount of sample fluid pressurized by  $N_2$  gas, which was separated from the sample fluid by a section of water, and (b) the distance (Y) of the sample position A (\*) from the methane–water interface in diffusion experiments. For details, see text. Taken from figure 3 of Chou et al. (2005).

and v-5 during Raman analysis, and check the sample pressure after analysis by opening v-3 (for low-pressure reading at G-1) or v-5 and v-4 (for high-pressure reading at G-2); (6) use the pressure generator or the exhaust valve (v-16) to reduce the sample pressure.

To load a sample of water or aqueous fluid at the enclosed end of the tube, use the following procedures: (1) remove the tube from the high-pressure valve; (2) heat the window section of the tube before dipping the open end of the tube in the sample solution; (3) after a sufficient amount of time to allow sample fluid to be sucked into the tube during cooling, force the sample solution to the enclosed end using a centrifuge; (4) reconnect the tube to the high-pressure valve and then it is ready for the evacuation and flushing procedures described above before pressurization with other fluids (Fig. 3b).

#### 2.3. Heating-cooling stages (USGS, INSTEC, Linkam)

The fused silica capillary in the HPOC can be prepared to a suitable length, such that the window section near the enclosed end can be inserted into a heating-cooling stage for *in situ* observations of samples at temperatures from near liquid nitrogen temperature ( $\sim$ -196°C) to 500 or 600°C at presussures up to 1000 bars. Three types of heating-cooling stage are commonly used and they are as follows: the USGS gas-flow stage, the INSTEC stage, and the Linkam CAP 500 stage. Because the USGS gas-flow stage has been described previously (Werre *et al.*, 1980) and because it is rather difficult to use for HPOC applications, it will not be discussed further here.

The INSTEC heating-cooling stage under a microscope of a JY LabRam 800 Raman system is shown in Figure 4, and the screen shows the two co-existing fluids in a FSCC. The stage was custom-designed for the HPOC and FSCC experiments and an mk1000 temperature controller and SN2-SYS liquid nitrogen cooling system were used to control sample temperatures in both the HPOC and FSCC. The sample holder of this stage has a sample slot (1 mm wide, 2.5 mm deep, and 40 mm long) located in the middle of a silver plate (43 mm  $\times$  16 mm  $\times$  2.5 mm), and a K-type thermocouple was inserted along the slot to monitor the sample temperatures (Fig. 5). A thin silica



Fig. 4. Photograph of an INSTEC heating-cooling stage and HORIBA JY HR 800 LabRam Raman system. The insert shows the stage under a microscope, and the screen shows the image of a meniscus separating two coexisting fluid phases in a FSCC (0.3 mm OD and 0.1 mm ID).

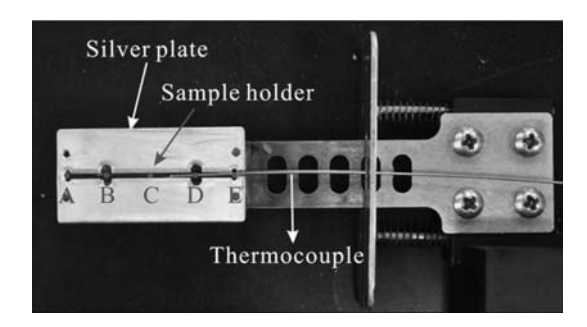


Fig. 5. A sample holder in the INSTEC heating-cooling stage with a slot  $(40 \text{ mm} \times 1 \times 2.5 \text{ mm})$  at the center of a silver plate  $(43 \text{ mm} \times 16 \text{ mm} \times 2.5 \text{ mm})$ . A FSCC up to 3 mm long can be placed in this slot. The enclosed end of fused silica capillary of a HPOC can also be inserted into the slot together with a Type-K thermocouple for direct sample-temperature measurements. Taken from figure 2b of Wang et al. (2011).

glass plate was mounted at the bottom part of the slot and an FSCC was placed in the slot and on top of the glass plate. For samples in the HPOC, the fused silica tube was inserted side by side with the thermocouple into the slot, and the sample near the closed end of the capillary tube was placed near the centre of the sample slot. The sample holder, together with sample (not shown) and thermocouple, were then inserted into the sample chamber of the stage, which has a  $60 \text{ mm} \times 40 \text{ mm}$  window (Fig. 6).

To investigate possible temperature gradients in the sample slot, target temperatures were set at 15, 30, 100, 200, 300 and 400°C, and the temperatures at five positions evenly distributed along the sample slot were measured with a K-type thermocouple (Fig. 5). The thermocouple was calibrated with the freezing and boiling points of pure water at ambient pressure at 0 and 100°C, respectively. As shown in Figure 7, at the target temperatures of 15 and 30°C, the temperature differences among different positions are  $<0.5^{\circ}$ C, which increased to  $\sim$ 2°C at the target temperature of 200°C.

The proto-type Linkam CAP 500 Capillary Pressure Stage (Fig. 8) was designed for the HPOC and FSCC and will soon be available on the market, after minor

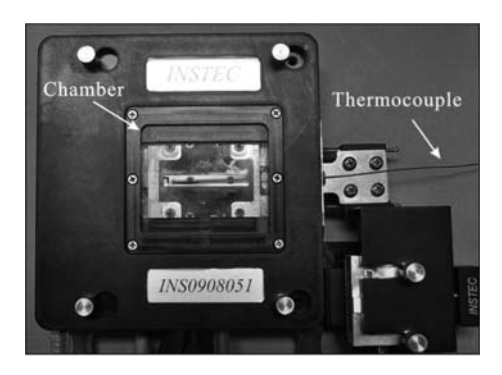
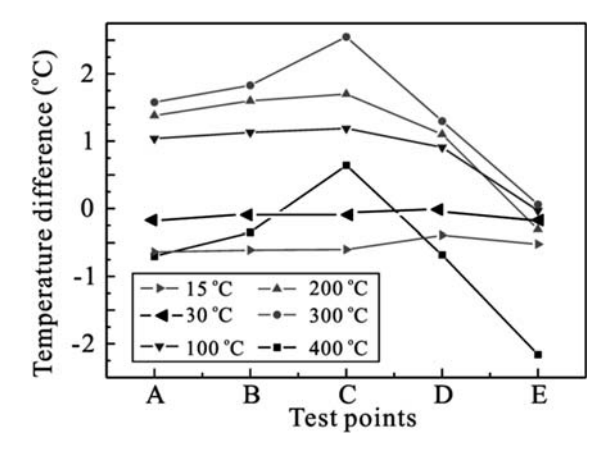
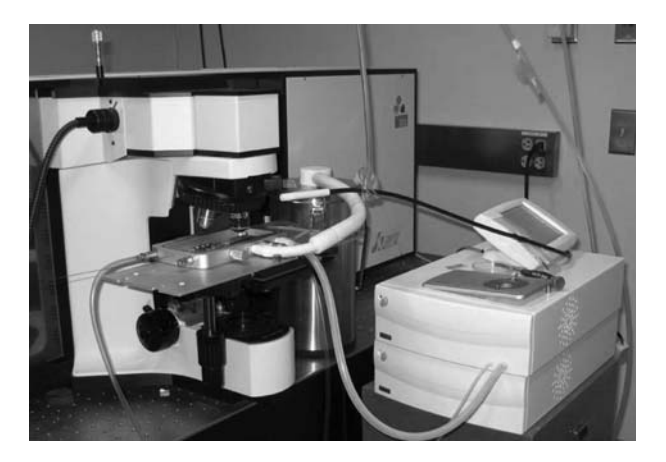


Fig. 6. INSTEC heating-cooling stage with a chamber area of  $60 \text{ mm} \times 40 \text{ mm}$  to show the whole silver plate of the sample holder. Taken from figure 2c of Wang et al. (2011).



*Fig.* 7. Temperature differences between sample and the set temperature of INSTEC temperature controller; the sample temperatures were measured with a calibrated type-K thermocouple and an Infinity digital meter at five positions evenly distributed along the sample holder (as shown in Figure 5). Taken from figure 2d of Wang *et al.* (2011).

modifications. Sample temperatures were controlled using a T95-PE system controller (http://www.linkam.co.uk/t95-system-controllers/) with a T95 LinkPad and LNP95 cooling system (http://www.linkam.co.uk/lnp95/) through Linksys32 temperature control and video capture software. The stage body can be water cooled by using an ECP (external circumferential piston) pump when heating samples above 300°C for >30 min. A capillary tube of HPOC being inserted into a channel (1 mm wide and 0.6 mm deep) of a silver block (20 mm wide and 50 mm long), is shown in Figure 9; the capillary can be moved 12.5 mm from the centre for a total 25 mm of movement.



*Fig. 8.* Photograph of a Linkam CAP 500 heating-cooling stage system, showing the temperature controller in the lower right corner, a dewar, and the stage (under the microscope).



*Fig. 9.* Photograph of the sample chamber of the Linkam CAP 500 heating-cooling stage. A fused silica capillary of an HPOC was inserted into the slot of a silver block under the microscope with the sample being positioned above a small hole at the centre of the silver block.

A small hole was drilled through the center of the silver block and its cover (photograph in Fig. 10), so that samples can be viewed with transmitted light. The silver block can be heated and cooled rapidly in the range -196 to  $500^{\circ}$ C at a rate from 0.1 to  $50^{\circ}$ C/min. The temperature sensor mounted in the silver block is a high-accuracy 100 ohm platinum resistor (to 1/10th Din Class A) and is accurate to  $0.1^{\circ}$ C. The block has been designed to minimize the temperature gradient along its length (Fig. 10).

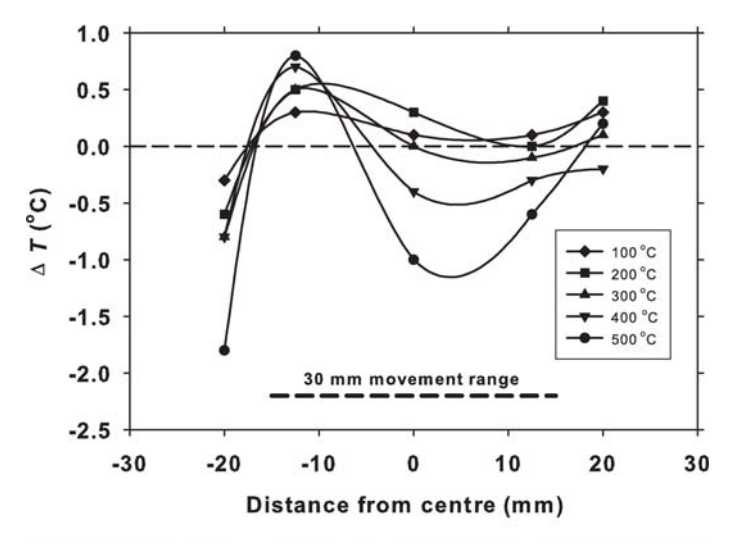
#### 2.4. Applications (examples)

#### 2.4.1. Solubility and diffusion of methane gas in water

Raman spectra of dissolved methane and water at five experimental positions with different distances (Y) away from the methane vapour/water interface (Fig. 3) collected  $\sim$ 240 min after the water was pressurized by methane at 35.47 MPa and 295.3 K are shown in Figure 11. The dissolved methane concentration in water at each Y can be calculated by using the measured peak area ratio between dissolved methane and water through the calibrated linear equation (Fig. 12; Lu *et al.*, 2006):

$$[X(CH_4)] = 1.0563[A(CH_4)_{aq}/A(H_2O)]$$
  $(R^2 = 0.9962)$  (1)

Raman peak-area ratios for CH<sub>4</sub>/H<sub>2</sub>O and concentrations of dissolved methane in water (in mole fraction, X, as calculated from equation 1) as a function of the distance between the sample spot and methane-water interface (Y, see Fig. 3) and time after the water was pressurized by methane at 24.47 MPa and 295.3 K are shown in Figure 13. The dotted curve represents the least-squares fit of the data at methane/water interface (Y = 0 mm). The solid curves represent calculated values for Y = 0.70, 4.12, 6.63, and 9.45 mm, assuming the left boundary condition is defined by the dotted curve and a diffusion coefficient (D) of 1.66 × 10<sup>-9</sup> m<sup>2</sup>s<sup>-1</sup> for methane in water. This diffusion coefficient gives the best fit of the observed concentration profiles (see Table VI and figure 7a of Lu *et al.*, 2006). As pointed out by Lu *et al.* (2006), this new spectroscopic method



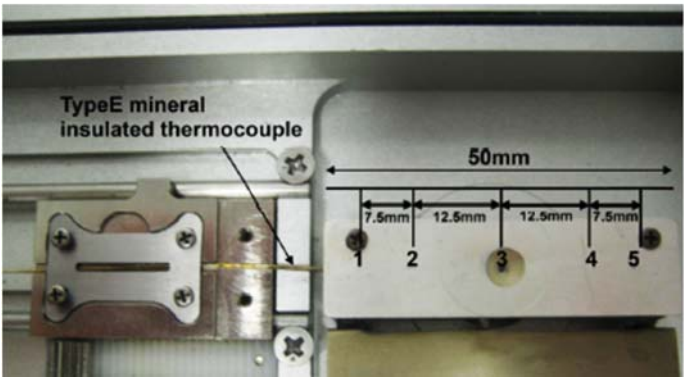
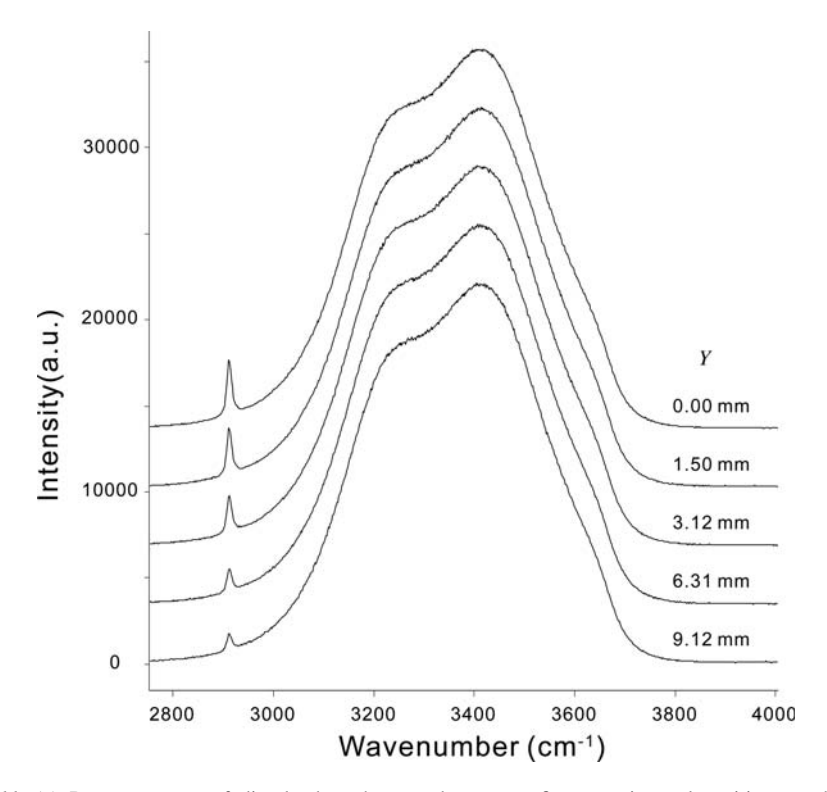


Fig. 10. Measured temperatures (with a type-E thermocouple) in a Linkam CAP 500 stage at five points (from 1 to 5) along the sample slot in a silver block under a silver cap, which has a hole at the centre allowing observations of samples with transmitted light. Each plotted data point shows the temperature difference between measured temperature (with thermocouple) and the set temperature. Image courtesy of Linkam Scientific Instruments Ltd.

investigates the diffusion under constant high pressure in a steady state, permitting the study of the pressure effect on diffusion.

This new method has several other advantages over existing methods, including: (1) the ability to directly monitor the methane-concentration variation in the water section with time and distance along the diffusion path, such that the diffusion process can be better understood, and a concentration-dependent diffusion rate can be derived from the concentration profile; (2) the method can be applied to all Raman-active species, such CO<sub>2</sub>, C<sub>2</sub>H<sub>6</sub>, N<sub>2</sub>, *etc.*, and can be extended to the investigation of multi-component diffusion in liquids as the concentration of each component in the solution can be obtained simultaneously; (3) this method shows its potential for studying more



*Fig. 11.* (a) Raman spectra of dissolved methane and water at five experimental positions at different distances (Y) from the methane vapour—water interface (Figure3b) collected  $\sim$ 240 min after the water was pressurized by methane at 35.72 MPa and 295.3 K. The intensity of the methane peak near 2910 cm<sup>-1</sup> decreases with increasing Y, indicating a concentration gradient of methane along the diffusion path in the cell. The spectra were collected with a  $40 \times$  long-working distance objective lens for  $40 \times$  with three accumulations. Taken from figure 5a of Lu *et al.* (2006).

complex systems when hydrate is present, in which the interaction of methane and water molecules might be different from the current metastable case, and the D might be more concentration dependent.

#### 2.4.2. Solubility of methane hydrate in water

Water (Lw) in equilibrium with SI methane hydrate (H) in HPOC at 276.55 K and 20 MPa is shown in Figure 14. Lu *et al.* (2008) collected Raman spectra of the water in equilibrium with SI methane hydrate at temperatures from 275.15 to 293.15 K and pressures of 10, 20, 30 and 40 MPa. Sixty measurements were made and the results can be represented by:

$$X(\text{CH}_4)(\pm 0.000095) = \exp[11.0464 + 0.023267P - (4886.0 + 8.0158P)/T]$$
 (2)

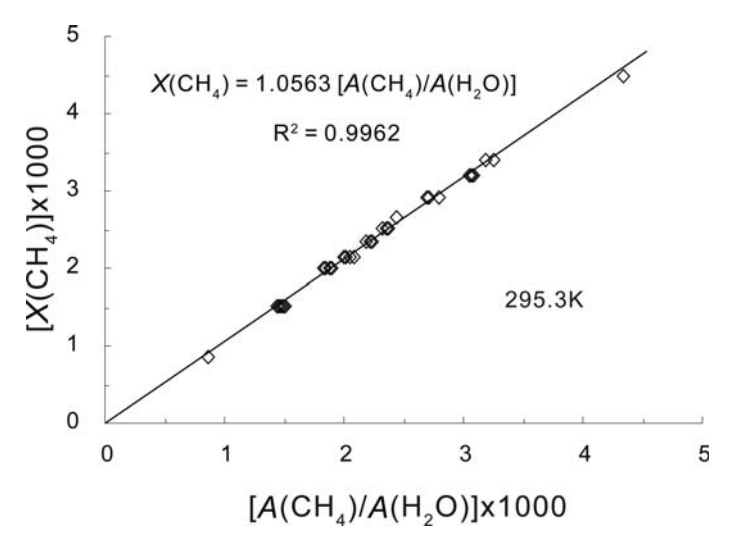


*Fig. 12.* Experimental results showing the linear relation between dissolved methane concentrations in water (in mole fraction, X(CH<sub>4</sub>)) and the peak-area ratios for aqueous methane and water at 295.3 K and different pressures (up to 47 MPa). The plotted data are from Table I of Lu *et al.* (2006). The straight line represents the linear regression of the experimental data. Taken from figure 4 of Lu *et al.* (2006).

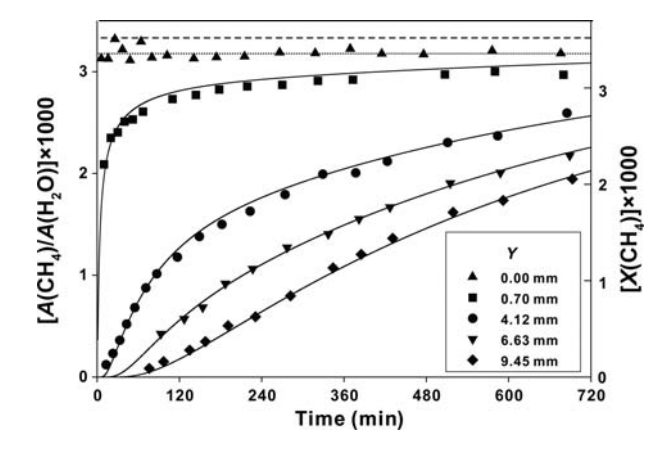


*Fig. 13.* Raman peak-area ratios for  $CH_4$ - $H_2O$  and the concentration of dissolved methane in water (in mole fraction, X, as calculated from equation 1) as a function of distance between the sample spot and the methanewater interface (Y, see Fig. 3) and time after the water was pressurized by methane at 24.47 MPa and 294.9 K. The dotted curve represents the least squares fit of the data at the methane–water interface (Y = 0 mm). The solid curves represent calculated values for Y = 0.70, 4.12, 6.63 and 9.45 mm, assuming the left boundary condition is defined by the dotted curve and a diffusion coefficient of  $1.66 \times 10^{-9}$  m<sup>2</sup> s<sup>-1</sup> for methane in water. This diffusion coefficient gives the best fit of the observed concentration profiles (Table VI and figure 7a of Lu *et al.*, 2006). The horizontal dashed line represents the equilibrium concentration of  $X_{CH_4} = 0.00352$ , which is slightly larger than the value shown by the dotted line. This difference resulted from the 0.6 K difference in temperature between the experiment and those experiments for defining the coefficient in equation 1. Each spectrum was collected for 40 s with three accumulations. Taken from figure 6a of Lu *et al.* (2006).

where P is pressure (MPa), and T is temperature (K). Equation 2 fits their measured data (their table 2) very well, with an average absolute deviation of 2.17% (their figure 8).

#### 2.4.3. Determination of methane vapour pressure with measured Raman shift

All the available data for the relation between measured methane  $v_1$  (C-H symmetric stretching) band positions and pressures near room temperature, including those of Lu *et al.* (2007) determined in HPOC are shown in Figure 15. The curves defined by each data set are nearly parallel to each other, indicating that systematic discrepancies among these data sets can be removed and a universal equation can be established by choosing D as a variable (Fig. 16), where  $D = v_p - v_o$ , the difference between the peak positions at elevated pressure  $(v_p)$  and near-zero pressure  $(v_o)$ :

$$P(\text{MPa}) = -0.0148 \times D^5 - 0.1791 \times D^4 - 0.8479 \times D^3$$
$$-1.765 \times D^2 - 5.876 \times D \tag{3}$$

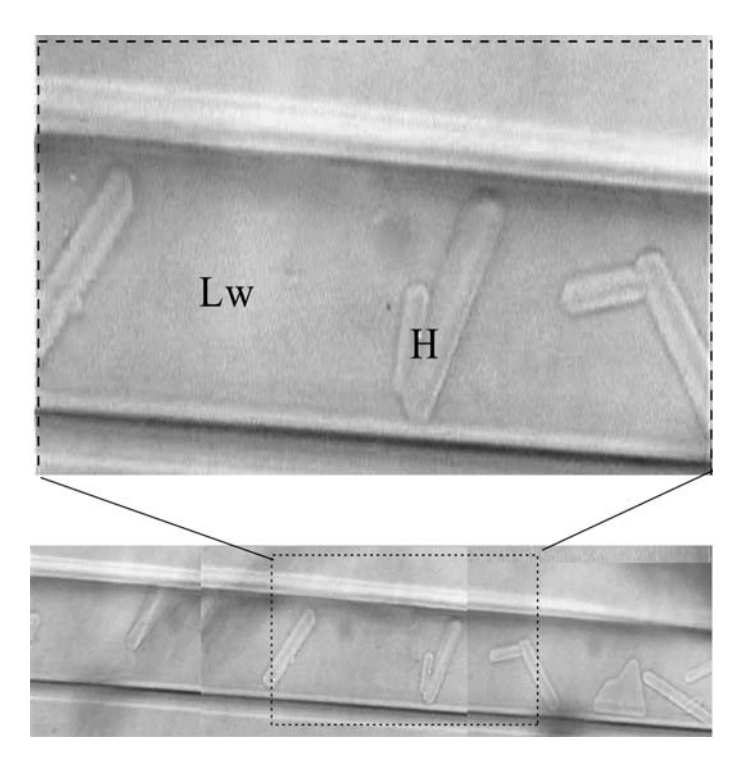


Fig. 14. Photographs of hydrate crystals in HPOC showing aqueous solutions (Lw) in equilibrium with sI methane hydrate (H) at 276.55 K and 20 MPa. Raman spectra were collected from the solution near the hydrate crystals. The width of the sample cavity is  $\sim$ 50  $\mu$ m. Taken from figure 3 of Lu et al. (2008).

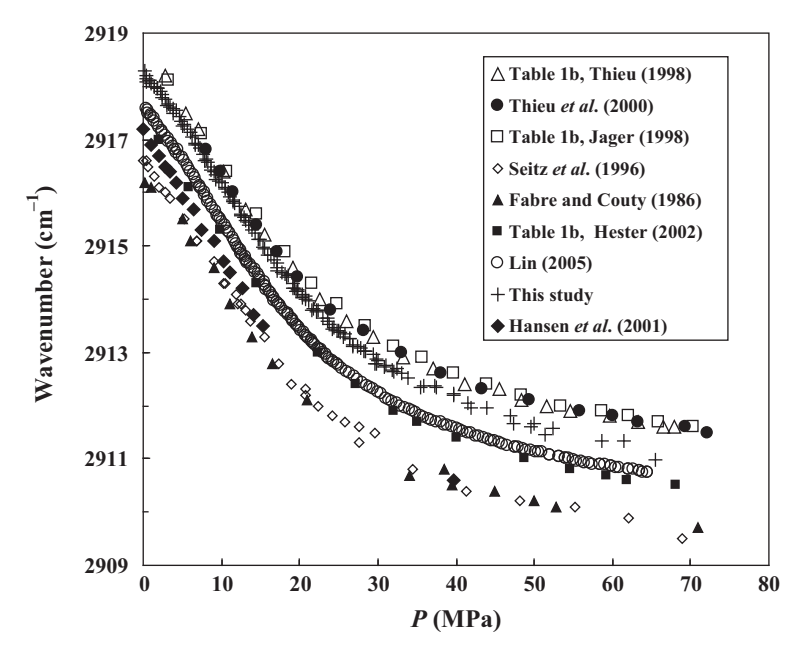


Fig. 15. Measured methane  $v_1$  (C-H symmetric stretching) band positions as a function of pressure, summarized by Lu *et al.* (2007). The near-parallel relationship for all experimental data sets indicates similar relations between pressure and Raman peak position, but with different intercepts at zero pressure. Taken from figure 1 of Lu *et al.* (2007).

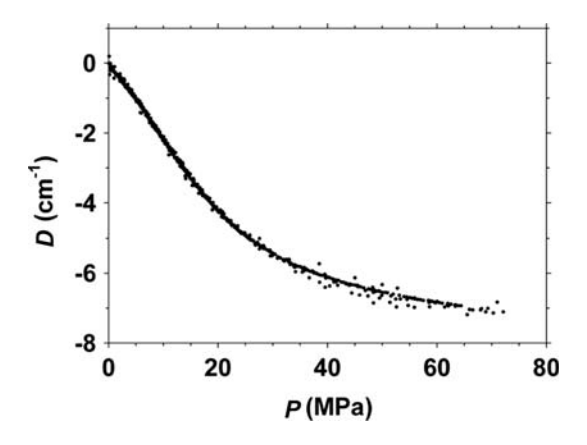
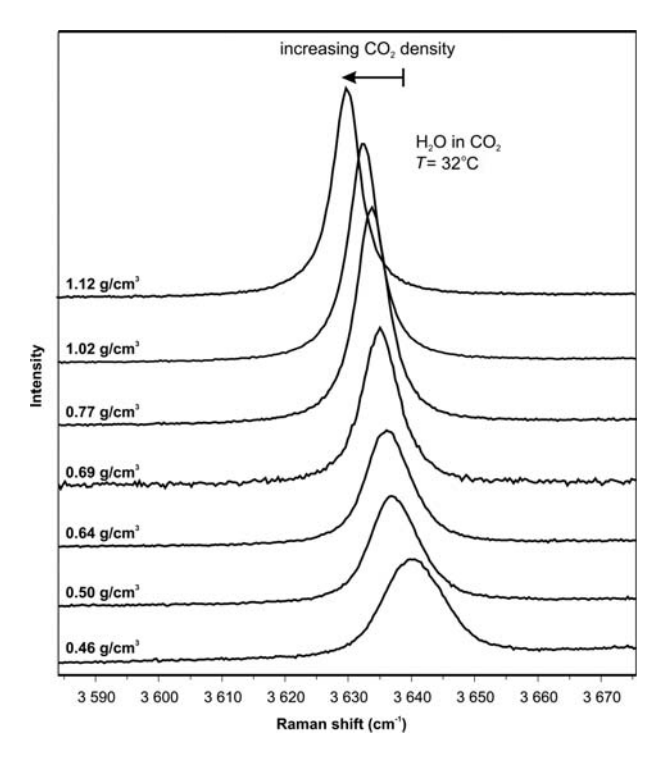


Fig. 16. The *P-D* relations for all data shown in Fig. 15, where  $D = v_p - v_o$ , the difference between the peak positions at elevated pressure  $(v_p)$  and near-zero pressure  $(v_o)$  for the methane  $v_1$  band, with  $v_o$  set at the values listed in Table 2 of Lu *et al.* (2007). Equation 3 represents all data points. Taken from figure 4 of Lu *et al.* (2007).

with  $R^2 = 0.9926$ . Therefore, equation 3 can be applied for calculating methane pressures (*P*) in sample fluids with measured Raman shifts of CH<sub>4</sub>  $v_1$  band position near room temperature, as long as  $v_0$  for the particular Raman spectrometer is known. This can be achieved by measuring directly the CH<sub>4</sub> peak position at pressures near zero in a HPOC (Chou *et al.*, 2005) or FSCC (Chou *et al.*, 2008a).

#### 2.4.4. Other applications

The examples given above are for  $CH_4$  gas or  $CH_4$  gas in pure water. These applications can be extended to other gases in saline water at different temperatures. Also, in HPOC, Raman spectra of various fluids and their mixtures can be collected at fixed pressures (up to  $\sim 1$  kbar) and temperatures (-196 to  $600^{\circ}C$ ) to show Raman spectroscopic characters of these fluids as a function of composition, total pressure and temperature. For instance, the effect of  $CO_2$  density on the symmetric stretching of dissolved  $H_2O$  is illustrated in Figure 17. Fluid standards of known composition and total pressure can be prepared in HPOCs as standards for quantitative Raman analyses of unknown samples and also for inter-laboratory comparison. Furthermore, compositions and total pressures of fluid standards in FSCCs can be determined by comparing Raman signals of these 'standards' with those in HPOC with known composition and total pressure.



*Fig.* 17. The evolution of the stretching frequency of water dissolved in CO<sub>2</sub> at 32°C as a function of CO<sub>2</sub> density saturated with respect to water (Berkesi *et al.*, 2009). Image courtesy of Jean Dubessy.

# 3. Fused silica capillary capsules (FSCCs)

#### 3.1. Construction of FSCCs

The fused silica capillaries used are similar to those for HPOC described in section 2.1, and the detailed description for the construction of FSCC was presented previously (Chou *et al.*, 2008a). Briefly, organic and inorganic samples in solid or liquid forms were first loaded into the tube,  $\sim$ 6 cm long with one end sealed. The tube was then centrifuged to force the sample towards the closed end. After centrifugation, the open end of the tube was connected to a pressure line (Fig. 18). After any air in the sample tube was evacuated through the pressure line, gaseous samples were then added cryogenically by immersing the sealed end of the tube in liquid nitrogen and switching the pressure line from vacuum to sample gas at  $\sim$ 0.2 MPa pressure. The gaseous component was allowed to condense or freeze to a solid for several minutes. The tube was evacuated and the open end was sealed by fusion in a hydrogen flame while the sample end remained frozen and under vacuum. For microthermometric measurements in a heating-cooling stage, the FSCCs <25 mm long were prepared (Fig. 19).

#### 3.2. Applications

#### 3.2.1. Calibration standards

Similar to the synthetic fluid inclusions trapped in quartz formed by healed fractures under a fixed P-T condition in the presence of fluid (Sterner and Bodnar, 1984), fluid samples in FSCCs can be used as standards for either temperature calibration of a heating-cooling stage or quantitative Raman spectroscopic analyses of fluid samples. For example, we have used the melting of  $H_2O$  ice at  $0^{\circ}C$ , ice in NaCl- $H_2O$  solution at  $-20.8^{\circ}C$ , solid  $CO_2$  at  $-56.6^{\circ}C$  (see figure 5 of Chou et~al., 2008a), and NaNO<sub>3</sub> at 306.8°C to calibrate our thermocouples. We prepared FSCC containing  $CH_4$  gas at a pressure near or below 1 atm., such that the peak position of  $v_1$  (C-H stretching

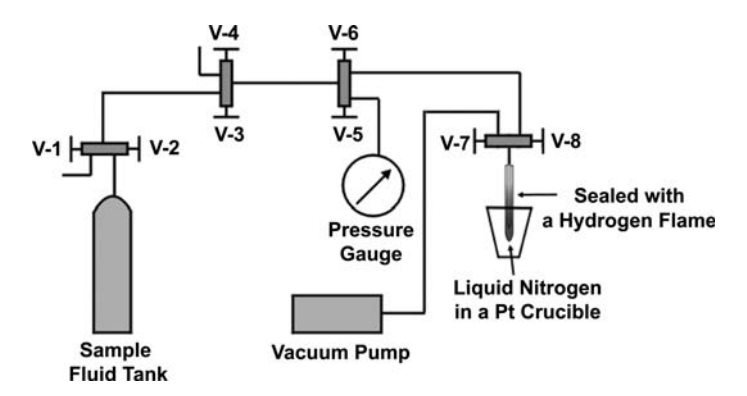


*Fig. 18.* A schematic diagram of the sample-loading system for a fused silica capillary capsule (FSCC). V-1 to V-8 are three-way/two-stem combination taper-seal valves from High Pressure Equipment Co. (Cat. No. 15-15AF1). For details, see the text. Taken from Chou *et al.* (2008a).

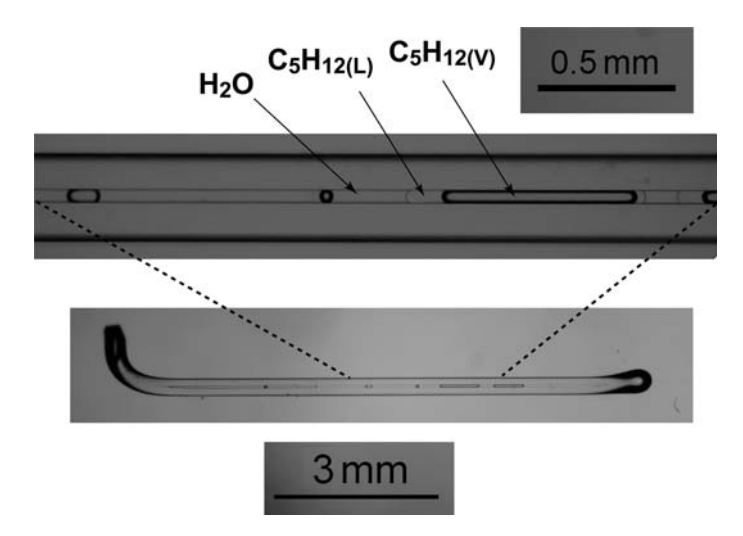


Fig. 19. A synthetic fluid inclusion in a fused silica capillary capsule with a square cross-section  $(0.3 \text{ mm} \times 0.3 \text{ mm})$  with a  $0.05 \text{ mm} \times 0.05 \text{ mm}$  cavity, and  $\sim 10 \text{ mm}$  long) containing liquid (L) and vapour (V) pentane ( $C_5H_{12}$ ) and water. The capsule is small enough to be fitted into the sample chamber of a heating-cooling stage for microthermometric analysis and/or in situ spectroscopic analysis at various P-T conditions. Taken from figure 2 of Chou et al. (2008a).

band) of methane near zero pressure ( $v_0$ ) can be determined for methane pressure measurements as described in section 2.4.3. We also prepared a FSCC containing pure  $CO_2$  with a bulk density near the critical density of  $CO_2$  (0.468 g/cm<sup>3</sup>), such that  $CO_2$  standards for the densities ranging from 0.014 to 1.179 g/ml can be obtained in this FSCC by fixing the temperatures of both liquid and vapour phases in a heating-cooling stage to within 0.1°C between -56.6 and 31.1°C (Fig. 20). By using these  $CO_2$  density standards in a FSCC, reliable  $CO_2$  densities in fluid samples can be determined by measuring the  $CO_2$  Fermi diad split as described by Wang *et al.* (2011) and references therein. Furthermore, we are developing methods for the preparation of gas standards in FSCCs with known compositions and pressures to be used in quantitative Raman spectroscopic analyses of gas samples (Chou *et al.*, 2011).

#### 3.2.2. Other applications

Many other applications of FSCCs were described by Chou *et al.* (2008a). FSCCs have been demosntrated as suitable cells for the study of speciation of uranyl ions in lithium chloride solutions using Raman spectroscopy as a function of temperature and chlorinity at saturation pressure, as shown by Dargent *et al.* (2011) (Fig. 21). FSCCs are particularly useful for studies of reactions of organic compounds in the presence or absence of water and also for systems containing sulphur at pressures up to 1 kbar and temperatures up to 600°C. Pyrolysis and hydrolysis of organic compounds and thermal chemical sulphate reduction (TSR) by hydrocarbons (Chou *et al.*, 2008b) are good examples.

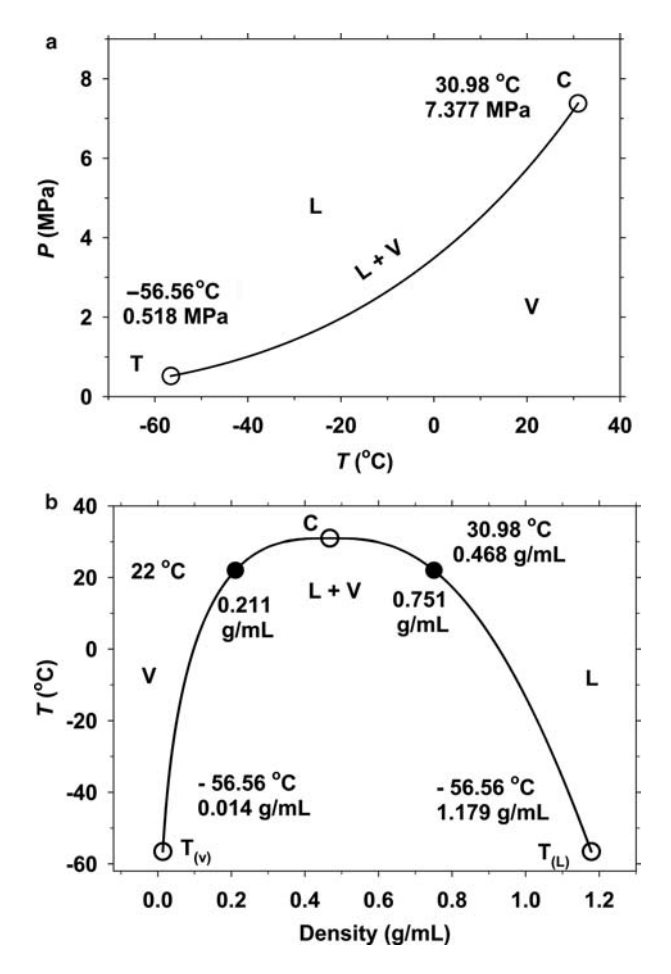


Fig. 20. Phase relations of a pure  $CO_2$  system, showing P-T relations for the L-V curve, the critical point (C), and triple point (T) in (a), and T-Density relations at  $22^{\circ}C$  and at C and T in (b).

Furthermore, the high permeability of fused silica to hydrogen makes it possible to control the redox state of a sample in a FSCC by an external hydrogen buffer in a gold capsule (Shang *et al.*, 2009) at relatively low temperatures ( $<400^{\circ}$ C).

# 4. Summary

Two types of optical cells with fused silica windows were described; the high-pressure optical cell (HPOC) and the fused silica capillary capsule (FSCC). Fluids of known compositions and pressures can be prepared in HPOC, and those enclosed in FSCC can be determined by comparing their Raman signals with those obtained from

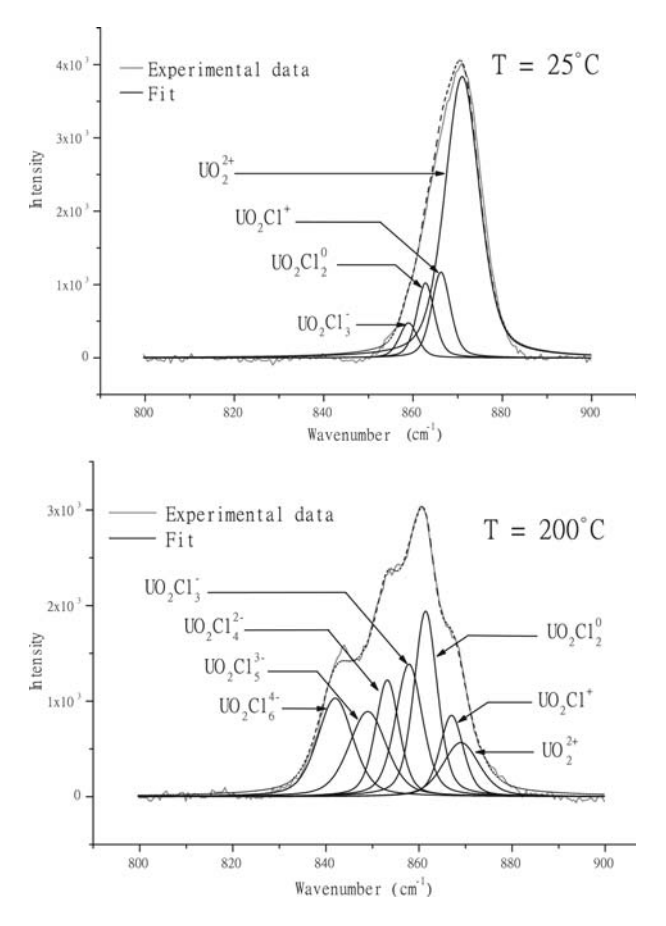


Fig. 21. Raman spectra of the symmetric vibrational mode of uranyl chloride complexes in LiCl solution (1.5 molal) at 25 and 200°C at vapour-saturation pressures (Dargent *et al.*, 2011). Image courtesy of Maxime Dargent.

samples prepared in HPOC. Because FSCCs are small (normally  $\sim$ 0.3 mm in diameter and <2.5 mm long), heating-cooling stages (USGS, INSTEC, or Linkam) can be used to control sample temperatures for *in situ* Raman analyses. FSCCs are also suitable for samples that need to be heated in furnaces with or without external pressure before Raman analyses of the quenched samples.

Even though the achieveable *P-T* conditions in HPOC and FSCC are quite limited when compared with those in HDAC, they have the following advantages for the study of geological fluids at *P-T* conditions up to 600°C and 1 kbar: (1) fluid samples which are easy to load; (2) easy to operate; (3) less expensive; (4) greater Raman signal intensity; and (5) sample pressures which can be measured directly when the HPOC is used.

Optical cells with fused silica windows are particularly suitable for the study of organic systems and for systems containing sulphur. Furthermore, fluid standards with known composition and pressure can be prepared in these types of cells for quantitative Raman analyses of either natural or synthetic fluids.

### Acknowledgments

The author is grateful to Jean Dubessy (UMR G2R, CNRS, Université de Lorraine, France) for his invitation to write this chapter, his review of it, and for providing two figures (17 and 21), and also to Bob Burruss (USGS), Yucai Song (Institute of Geology, Chinese Academy of Geological Sciences), Wanjun Lu (China University of Geosciences at Wuhan), Xiaolin Wang (Nanjing University), Shunda Yuan (Institute of Mineral Resources, Chinese Academy of Geological Sciences), and Linbo Shang (Institute of Geochemistry, Chinese Academy of Sciences) for their help with the development of experimental techniques. Linkam Scientific Instruments Ltd. and Maxine Dargent (Université Henri Poincaré, France) provided Figures 10 and 21, respectively. Critical reviews by Harvey Belkin (USGS) and Guoxiang Chi (University of Regina, Canada) improved the presentation. The use of trade, product, industry, or firm names in this report is for descriptive purposes only and does not constitute endorsement by the U.S. Government.

#### References

- Berkesi, M., Hidas, K., Guzmics, T., Dubessy, J., Bodnar, R.J., Szabó, C., Vajna, B., Pintér, Zs. & Tsunogae, T. (2009) Presence of H<sub>2</sub>O in deep lithospheric fluid inclusions: a combined method of Raman spectroscopy and heating-freezing stage. In: *European Current Research on Fluid Inclusions (Granada, Spain), Programme and Abstracts*, pp. 29–30.
- Chou, I-M., Pasteris, J.D. & Seitz, J.C. (1990) High-density volatiles in the system C-O-H-N for the calibration of a laser Raman microprobe. *Geochimica et Cosmochimica Acta*, **54**, 535–543.
- Chou, I-M., Burruss, R.C. & Lu, W.J. (2005) A new optical cell for spectroscopic studies of geologic fluids at pressures up to 100 MPa. In: *Advances in High-Pressure Technology for Geophysical Applications* (J. Chen, Y. Wang, T.S. Duffy, G. Shen & L.F. Dobrzhinetskaya, editors). Elsevier, Amsterdam, pp. 475–485.
- Chou, I-M., Song, Y.C. & Burruss, R.C. (2008a) A new method for synthesizing fluid inclusions in fused silica capillaries containing organic and inorganic material. *Geochimica et Cosmochimica Acta*, 72, 5217–5231.
- Chou, I-M., Shang, L.B. & Burruss, R.C. (2008b) Thermochemical sulfate reduction (TSR) by methane in situ observation and Raman characterization in fused silica capsules at temperatures up to 450°C. In: *Fall Meeting of American Geophysical Union (San Francisco), Abstract*, P43B–1402.
- Chou, I-M., Lu, W.J., Chi, G.X. & Burruss, R.C. (2011) Calibrating Raman spectroscopic systems for quantitative analysis of geological fluids using standards prepared in fused silica capillaries. In: *Annual Meeting of Geological Society of America, (Minneapolis, Minnesota), Abstracts*, A89–6.
- Dargent, M., Dubessy, J., Caumon, M.-C. & Trung, C.-N. (2011) Etude de la spéciation de l'uranyle par spectroscopie Raman dans des solutions chlorurées (LiCl = 0,5 à 15 m) jusqu'à 350°C. Conséquences métallogéniques et perspectives. Réunion de la Société Géologique de France, Géologie et Chimie de l'Uranium.

- Fabre, D. & Couty, R. (1986) Etude, par spectroscopie Raman, du methane comprimé jusqu à 3 kbar. Application à la mesure de pression dans les inclusions continues dans les minéraux. Académie des Sciences, Paris. Comptes Rendus, 303, 1305–1308.
- Fall, A., Tattitch, B. & Bodnar, R.J. (2001) Combined microthermometric and Raman spectroscopic technique to determine the salinity of H<sub>2</sub>O-CO<sub>2</sub> -NaCl fluid inclusions based on clathrate melting. *Geochimica et Cosmochimica Acta*, 75, 951–964.
- Hansen, S.B., Berg, R.W. & Stenby, E.H. (2001) Raman spectroscopic studies of methane—ethane mixtures as a function of pressure. *Applied Spectroscopy*, **55**, 745–749.
- Hester, K. (2002) Three independent sets of measurements of methane  $v_1$  band positions at elevated pressures determined at the Center for Hydrate Research, Colorado School of Mines. Personal communication, published in Table 1b of Lu *et al.* (2007).
- Irish, D.E., Jarv, T. & Ratcliffe, C.I. (1982) Vibrational spectral studies of solutions at elevated temperatures and pressures. III. A furnace assembly for Raman spectral studies to 300°C and 15 MPa. *Applied Spectroscopy*, **36**, 137–140.
- Jager, M. (1998) Three independent sets of measurements of methane  $v_1$  band positions at elevated pressures determined at Center for Hydrate Research, Colorado School of Mines. Personal communication, published in Table 1b of Lu *et al.* (2007).
- Lin, F. (2005) Experimental Study of the PVTX Properties of the system H<sub>2</sub>O-CH<sub>4</sub>. PhD dissertation, Virginia Polytechnic Institute and State University, Virginia, USA.
- Lin, F., Bodnar, R.J. & Becker, S.P. (2007) Experimental determination of the Raman CH<sub>4</sub> symmetric stretching ( $\nu_1$ ) band position from 1–650 bar and 0.3–22°C: Application to fluid inclusion studies. *Geochimica et Cosmochimica Acta*, **71**, 3746–3756.
- Lu, W.J., Chou, I-M., Burruss, R.C. & Yang, M.Z. (2006) In-situ study of mass transfer in aqueous solutions under high pressures via Raman spectroscopy: A new method for the determination of diffusion coefficients of methane in water near hydrate formation conditions. *Applied Spectroscopy*, **60**, 122–129.
- Lu, W.J., Chou, I-M., Burruss, R.C. & Song, Y.C. (2007) A unified equation for calculating methane vapor pressures in CH<sub>4</sub>-H<sub>2</sub>O system with measured Raman shifts. *Geochimica et Cosmochimica Acta*, 71, 3969-3978.
- Lu, W.J., Chou, I-M. & Burruss, R.C. (2008) Determination of methane hydrate solubility in the absence of vapor phase by in-situ Raman spectroscopy. *Geochimica et Cosmochimica Acta*, **72**, 412–422.
- Schmidt, C. & Chou, I-M. (2012) The hydrothermal diamond anvil cell (HDAC) for Raman spectroscopic studies of geologic fluids at high pressures and temperatures. In: *Applications of Raman Spectroscopy to Earth Sciences and Cultural Heritage* (J. Dubessy, M.-C. Caumon & F. Rull, editors). EMU Notes in Mineralogy, **12**. European Mineralogical Union and the Mineralogical Society of Great Britain and Ireland, pp. 249–278.
- Seitz, J.C., Pasteris, J.D. & Chou, I-M. (1993) Raman spectroscopic characterization of gas mixtures. I. Quantitative composition and density determination of CH<sub>4</sub>, N<sub>2</sub>, and their mixtures: American Journal of Science, 293, 297–321.
- Seitz, J.C., Pasteris, J.D. & Chou, I-M. (1996) Raman spectroscopic characterization of gas mixtures. II. Quantitative composition and pressure determination of the CO<sub>2</sub>-CH<sub>4</sub> system. *American Journal of Science*, 296, 577–600.
- Shang, L.B., Chou, I-M., Lu, W.J., Burruss, R.C. & Zhang, Y.X. (2009) Determination of diffusion coefficients of hydrogen in fused silica between 296 and 523 K by Raman spectroscopy and application of fused silica capillaries in studying redox reactions. *Geochimica et Cosmochimica Acta*, 73, 5435–5443.
- Sterner, S.M. & Bodnar, R.J. (1984) Synthetic fluid inclusions in natural quartz. I. Compositional types synthesized and applications to experimental geochemistry. *Geochimica et Cosmochimica Acta*, 48, 2659–2668.
- Thieu, V. (1998) Three independent sets of measurements of methane  $v_1$  band positions at elevated pressures determined at Center for Hydrate Research, Colorado School of Mines. Personal communication, published in Table 1b of Lu *et al.* (2007).
- Thieu, V., Subramanian, S., Colgate, S.O. & Sloan, E.D. Jr. (2000) High-pressure optical cell for hydrate measurements using Raman spectroscopy. In: *Gas Hydrates, Challenges for the Future* (G.D. Holder

- & P.R. Bishnoi, editors). Vol. 912 of the Annual Report of the New York Academy of Science, pp. 983–992.
- Wang, X.L., Chou, I-M., Hu, W.X., Burruss, R.C., Sun, Q. & Song, Y.C. (2011) Raman spectroscopic measurements of CO<sub>2</sub> density: Experimental calibration with high-pressure optical cell (HPOC) and fused silica capillary capsule (FSCC) with application to fluid inclusion observations. *Geochimica et Cos-mochimica Acta*, 75, 4080–4093.
- Werre, R.W. Jr., Bodnar, R.J., Bethke, P.M. & Barton, P.B. Jr. (1980) Novel heating-freezing fluid inclusion stage. U. S. Geological Survey Professional Paper, 1175, 190 pp.